Contents

List of Figures

List of Tables

Chapter 1

Introduction

The retrieval of snow depth information from passive microwave brightness temperature is very important to the geophysical study of Arctic areas. Its high albedo greatly impacts the global radiation balance due to its positive feedback to the climate change. If the climate becomes warmer, the snow is melted which decreases the reflected solar radiation and in turn the climate will become even warmer. On the other hand, colder climate leads to more snow which makes the climate more cooler. And the water content represented by the snow packs is a key variable of the hydrological cycle. The melting snow is the input of freshwater which changes the salinity of the ocean. The snow cover also dramatically changes the microwave signature of the beneath sea ice. The ice concentration estimation thus suffers from errors if excluding the snow packs covering. For all these reasons, it is neccessary to obtain the seasonal and geographical distribution of the snow depth on high altitude areas.

The current snow depth retrieval can be divided into three categories.

1. Retrieval methods by means of the brightness temperature gradient. This kind of method takes use of the scattering difference under various frequency bands while neglecting the inner physical characteristics of the snow pack. They can only used on the first year (FY) ice because of the microwave signature resemblance of snow and multiple year (MY) ice. The physical change of the snow will then result in errors in the snow depth estimation. The effect of snow grain size and density on the snow depth retrieval is discussed in Markus's paper[ref].

2. Retrieval methods using empirical/semi-empirical models like the HUT model[ref]. HUT model is the thermal emission model developed for the applications of snow covered terrain by Helsinki University of Technology. The effects of forest canopy and the soil on the brightness temperature is estimated by empirical or semi empirical formulas. The snow is considered to be a whole layer. The forward scattering of snow

is a constant and the extinction coefficient is a function of the grain size and the frequency. HUT thus can't handle the vertical change of the snow packs and its use under high frequencies should be more careful due to the shallow penetration depth which is less than the snow depth.

3. Retrieval methods using fully parametrized emission model for snow like MEMLS. MEMLS stands for the microwave emission model of layered snowpacks. The snowpacks are inhomogeneous and strongly layered. Noticeable change on brightness temperature will occur even for slight change of the absorption and scattering coefficients. It is more physically and radiometrically correct for the snowpacks to be processed in the structure of layers which characterized by the individual layer density, grain size, physical temperature, water content and depth. MÃď tzler [ref] shows that MEMLS correctly stimulates the brightness temperature of snow on the black body and on metal plate. Rasmus Tanboe extends MEMLS to the application on sea ice [ref]. The advantage of MEMLS for the snow cover lies not only on its correct brightness temperature simulation, but also on its realistic reflection of the snow characteristics which mark the meteorological changes in the history.

Three kinds of data set classified by the spatial resolution can be used for snow depth retrieval of Arctic area :

1. Surfaced based measurements. The spatial resolution is between 1 to 2 meters. Accurate local microwave signature can be achieved and interpreted along with the physical properties of the location.

2. Aircraft based measurements. The spatial resolution is between 10 to 100 meters. Various ice type and ice features can be captured in the radiometric signature.

3. Satellite based measurements. The spatial resolution is between 15 to 30 km. The areal variation can not be detected. While the ice concentration and ice type can be well determined by its large footprint scale. The large footprint also demands a general emission model for the snow covered ice. MEMLS as a model devoid of any free parameters is then suitable to stimulate the brightness temperature contribution at the surface.

[Followed by a brief introduction of what each chapter deals with.]

Chapter 2

Emission model

In this chapter, a sandwich layering model is analyzed and compared using two different methods. An extension of multiple layers is followed.

2.1 Sandwich emission model

Considering the case of three layers, with the air on the top, snow layer in the middle and ice at the bottom. Two methods are applied to show the effect of dielectric constants on upwelling brightness temperature above the top layer.
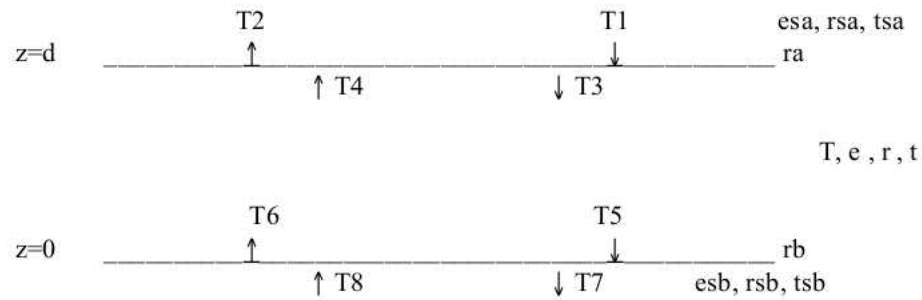
2.1.1 Method used by MEMLS

Figure 2.1: Sandwich model of a plane parallel snow slab with thickness d, illuminated by brightness temperature T1 from above and by T8 from below, emitting T2 upwards and T7 downwards (Source: Fig 1 in Note 1)

As Fig. 2.1 shows, air locates above $z = d$ plane and the ice locates beneath the $z = 0$ plane. The snow slab is at the middle. The emissivity of the snow layer has an internal emissivity of e, transmissivity of t and reflectivity

6

of r. And T is the physical temperature of snow layer. Th reflectivity at air-snow and snow-ice interface is r_a r_b respectively. esa, rsa, tsa is the total emissivity ,reflectivity and total transmissivity when illuminated from above. And esb, rsb, tsb is the total emissivity ,reflectivity and total transmissivity when illuminated from below. Assuming T is zero, the internal brightness temperature relates with the external temperature as the following:

$$T2 = raT1 + (1 - ra)T4;$$
$$T3 = (1 - ra)T1 + raT4;$$
$$T4 = rT3 + tT6;$$
$$T5 = tT3 + rT6;$$
$$T6 = rbT5 + (1 - rb)T8;$$
$$T7 = (1 - rb)T5 + rbT8;$$

On the case of $T \neq 0$, the emission contribution should be included. Now the brightness temperature T_2 can be computed as:

$$T_2 = rsaT_1 + esaT + tsT_8$$

T is the physical temperature of snow. rsa can be computed using the e, r, t of each layer and the interface reflectivity rsa and rsb:

$$rsa = ra + (1 - ra)^2 roa/(1 - ra.roa)$$
$$rsb = rb + (1 - rb)^2 rob/(1 - rb.rob)$$
$$ts = tsa = tsb = t(1 - ra)(1 - rb)/((1 - r.ra)(1 - rb) - ra.rb.t^2)$$

where roa and rob is:

$$roa = r + rb.t^2/(1 - r.rb)$$
$$rob = r + ra.t^2/(1 - r.ra)$$

The refractive index $n = n' + in''$ can be calculated from the dielectric constant $\epsilon = \epsilon_1 + i\epsilon_2$:

$$n' = \sqrt{\frac{\sqrt{\epsilon_1^2 + \epsilon_2^2} + \epsilon_1}{2}}$$

$$n'' = \sqrt{\frac{\sqrt{\epsilon_1^2 + \epsilon_2^2} - \epsilon_1}{2}}$$

When $\epsilon_1 \gg \epsilon_2$, $n = n' = \sqrt{\epsilon_1}$.

The interface reflectivity of horizontal and vertical polarization then can be found by the Snell's law and Fresnel equation. At the air-snow interface,

$$ra_h = \left[\frac{n_1 cos(\theta_i) - n_2 cos(\theta_t)}{n_1 cos(\theta_i) + n_2 cos(\theta_t)}\right] = \left[\frac{n_1 cos\theta_1 - n_2\sqrt{1 - (\frac{n_1}{n_2}sin\theta_1)^2}}{n_1 cos\theta_1 + n_2\sqrt{1 - (\frac{n_1}{n_2}sin\theta_1)^2}}\right]^2$$

$$ra_v = \left[\frac{n_1 cos(\theta_t) - n_2 cos(\theta_i)}{n_1 cos(\theta_t) + n_2 cos(\theta_i)}\right] = \left[\frac{n_2 cos\theta_1 - n_1\sqrt{1 - (\frac{n_1}{n_2}sin\theta_1)^2}}{n_2 cos\theta_1 + n_1\sqrt{1 - (\frac{n_1}{n_2}sin\theta_1)^2}}\right]^2$$

And at the snow-ice interface, n_1 and n_2 is the refractive index of snow and ice respectively. And the incidental angle θ_2 is:

$$\theta_2 = \arcsin\frac{sin\theta_1}{n_{snow}}$$

As for the layer internal parameters, the internal radiative-transfer equation
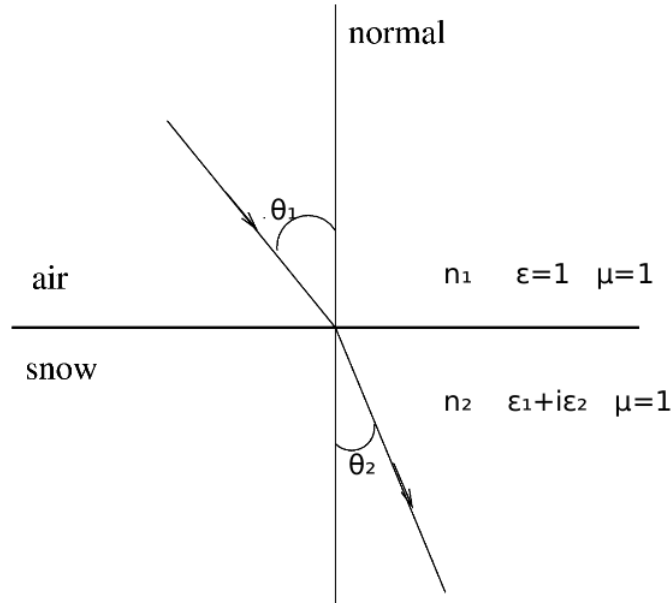

Figure 2.2: Reflection at air-snow interface

describes how radiation (T4 to T6 in Fig 2.1) is modified when it propagates over a path. The radiance is increased by emission and reduced by absorption. Considering the 6-flux radiative model showed in figure Fig 2.3. All the horizontal fluxes are the same. The vertical fluxes is:

$$\frac{dT_1}{dz}|cos\theta| = \gamma_a(T_1 - T) + \gamma_b(T_1 - T_2)$$
$$\frac{dT_2}{dz}|cos\theta| = -\gamma_a(T_2 - T) - \gamma_b(T_1 - T_2)$$

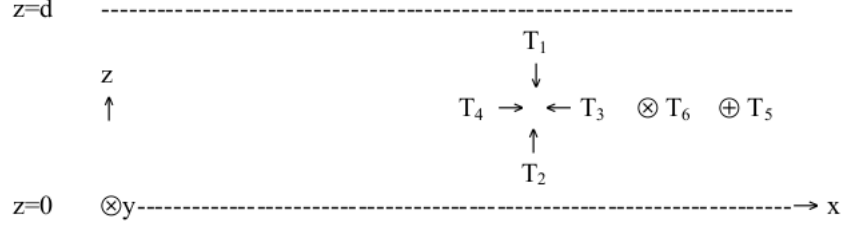where γ_a is the absorption coefficients and γ_b is the scattering coefficients.

Figure 2.3: Six fluxes inside the snow layer(Source: Note 2 Fig.1)

The total reflectivity, emissivity and transmissivity can be calculated by γ_a and γ_b:

$$r = \frac{r_0(1 - t_0{}^2)}{1 - r_0{}^2 t_0{}^2}$$
$$t = \frac{t_0(1 - r_0{}^2)}{1 - r_0{}^2 t_0{}^2}$$
$$r_0 = \frac{\gamma_b}{\gamma_a + \gamma_b + \gamma}$$
$$\gamma = \sqrt{\gamma_a(\gamma_a + 2\gamma_b)}$$
$$t_0 = e^{-\gamma d/|cos\theta|}$$

where γ is the damping coefficient.

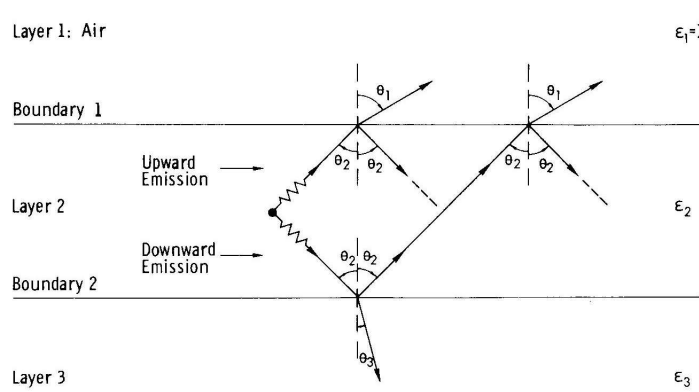## 2.1.2   Impedance matching

Figure 2.4: Emission by layer 2 into layer 1 (Source: Ulaby. Microwave remote sensing. vol1. Fig 4.24)

Another way to analyze the sandwich model is by means of impedance matching. Considering the incoherent case where the profile has a continuous

dielectric constant, the upwelling brightness temperature is contributed from emission from snow and ice layer:

$$T_B = T_{B2} + T_{B3}$$

And the emission from each layer is the sum of the downward emitted radiation T_D and upward emitted T_D which is illustrated on Fig.2.4. Including all the multiple reflections as showed in Fig.??, the contributions from snow and ice into air is computed.

The upward emitted radiation from snow layer is:

$$T_{2U} = (1 - \Gamma_1)T_{S2} + (1 - \Gamma_1)\frac{\Gamma_1\Gamma_2}{L_2^2}T_{S2} + ...$$

$$= (1 - \Gamma_1)T_{S2}[1 + x + x^2 + ...]$$

where $x = \frac{\Gamma_1\Gamma_2}{L_2^2}$ The reflectivity at the air-snow and snow-ice interface Γ_1 Γ_2 is decided by the intrinsic impedance.

$$\Gamma_1 = |\frac{Z_{snow} - Z_{air}}{Z_{snow} + Z_{air}}|^2 \Gamma_2 = |\frac{Z_{ice} - Z_{snow}}{Z_{ice} + Z_{snow}}|^2$$

The intrinsic impedance of each layer is:

$$Z_h = \sqrt{\frac{\mu_r}{\epsilon_r}}cos\theta$$

$$Z_v = \sqrt{\frac{\mu_r}{\epsilon_r}}sec\theta$$

The loss factor of snow layer L_2 is:

$$L_2 = e^{2\alpha dsec\theta_2}$$

where $\alpha = \frac{2\pi}{\lambda_0}Im\sqrt{\epsilon}$ and d is the thickness of snow layer. The total energy received at air-snow interface by snow layer is:

$$T_{S2} = (1 - a_2)T_2(1 - \frac{1}{L_2})$$

where T_2 is the physical temperature and a_2 is the single-scattering albedo. Because Γ_1 Γ_2 is smaller than one and loss factor is larger than one, $x < 1$, the sum has a closed form:

$$T_{2U} = \frac{(1 - \Gamma_1)T_{S2}}{1 - \Gamma_1\Gamma_2/L_2^2}$$

The downward emitted radiation from snow layer is:

$$T_{2D} = \frac{\Gamma_2(1 - \Gamma_1)T_{S2}}{L_2} + \frac{\Gamma_2^2\Gamma_1(1 - \Gamma_1)T_{S2}}{L_2^3} + \frac{\Gamma_2^3\Gamma_1^2(1 - \Gamma_1)T_{S2}}{L_2^5} + ...$$

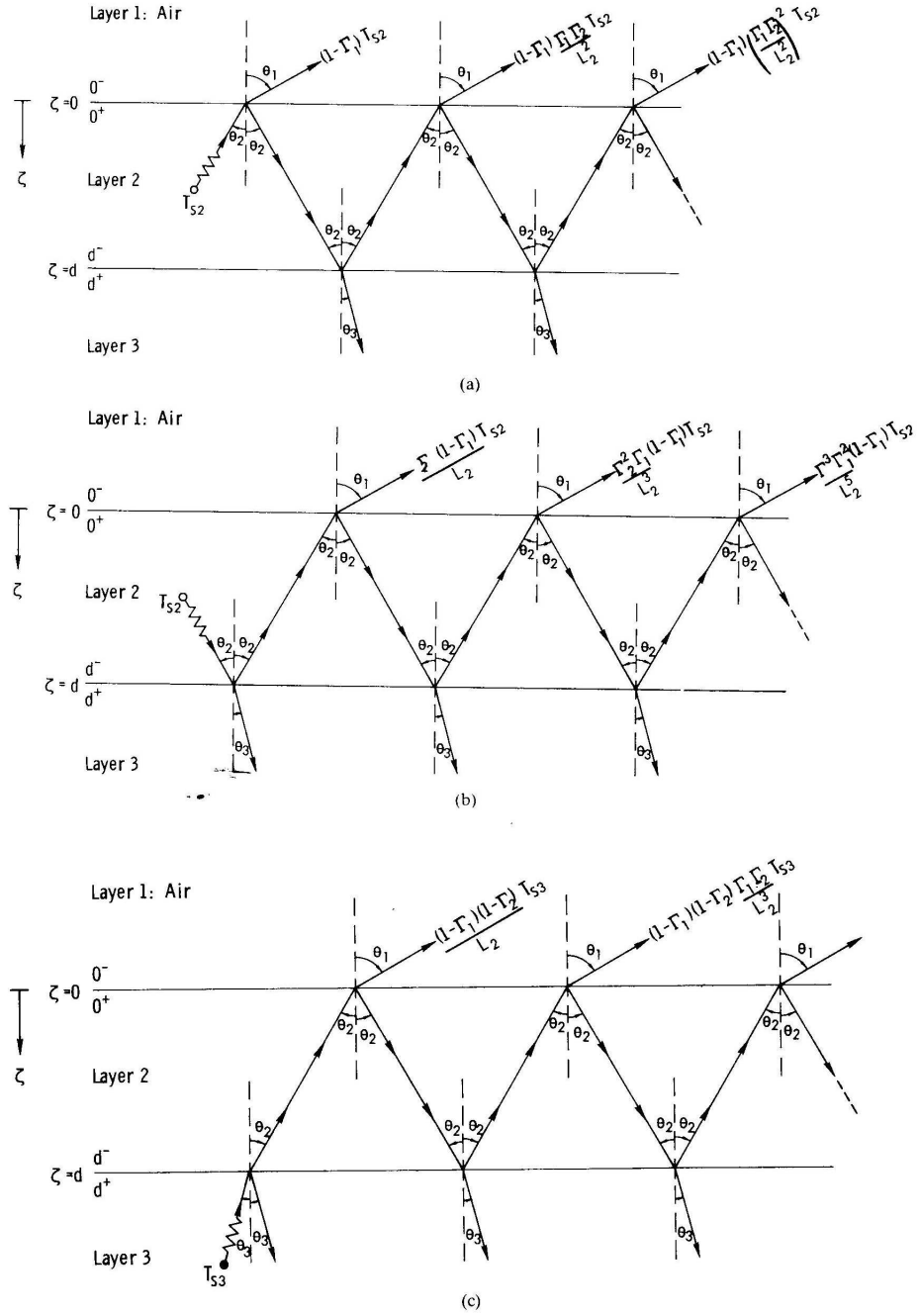$$= \frac{\Gamma_2(1 - \Gamma_1)T_{S2}}{L_2}(1 + x + x^2 + ...)$$

Figure 2.5: (a) Upward emission from snow layer T_{2U};(b) Downward emission from snow layer T_{2D};(c) Downward emission from ice layer T_{3U}(Source: Ulaby. Microwave remote sensing. vol1. Fig 4.25)

Likewise, the closed form is:

$$T_{2D} = \frac{\Gamma_2(1 - \Gamma_1)T_{S2}}{L_2(1 - \Gamma_1\Gamma_2/L_2^2)}$$

The radiation contribution from ice only includes upward emitted radiation assuming that the ice has semi-infinite depth in which case

$$T_{S3} = T_3$$

where T_3 is the physical temperature of ice. The radiation contribution from ice is then given as:

$$T_{B3} = \frac{(1 - \Gamma_1)(1 - \Gamma_2)T_3}{L_2(1 - \Gamma_1\Gamma_2/L_2^2)}$$

Summing all the contribution together, the upwelling brightness temperature at the air-snow interface is:

$$T_B = \left(\frac{1 - \Gamma_1 T_3}{1 - \Gamma_1\Gamma_2/L_2^2}\right)\left[\left(1 + \frac{\Gamma_2}{L_2}\right)\left(1 - \frac{1}{L_2}\right)(1 - a)T_2 + \frac{1 - \Gamma_2}{L_2}T_3\right]$$

2.1.3 Comparison

Excluding the scattering in the above two methods and assuming the sky radiance is zero which leads to $\gamma = 2\alpha$ $T_1 = 0$ and $a_2 = 0$, it can be derived that:

$$TB_{MEMLS} = \left(\frac{1 - \Gamma_1 T_3}{1 - \Gamma_1\Gamma_2/L_2^2}\right)[(1 + \Gamma_2 t)(1 - t)T_2 + t(1 - T_2)T_3]$$
$$= TB_{impedance}$$

where $t = t_0 = e^{-\gamma d sec\theta_2}$. Fig. 2.6 is curve of brightness temperature by the permittivity of the snow. As expected, the two methods give the identical curve. The dielectric of ice is $\epsilon = 3.2 + i0.5$. The depth of the snow layer is 20cm. The physical temperature of snow and ice layer is 250K and 270K respectively. The permittivity of the snow varies from 1.4 to 3.2. Upwelling brightness temperature reduces with larger permittivity which shows the reflection happened at the snow-ice interface is more dominant of the radiation contribution. The decreasing value of H channel is about 40K within the permittivity range while the V channel hardly changes with the permittivity.
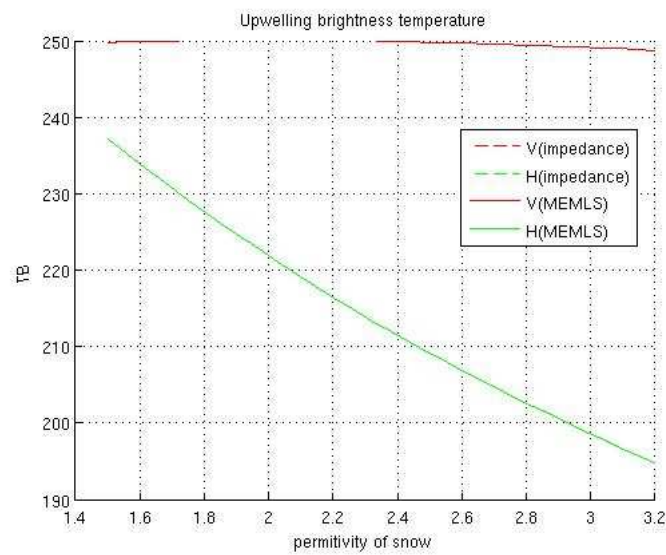
Figure 2.6: Upwelling temperature vs. permittivity of snow with impedance matching and MEMLS method
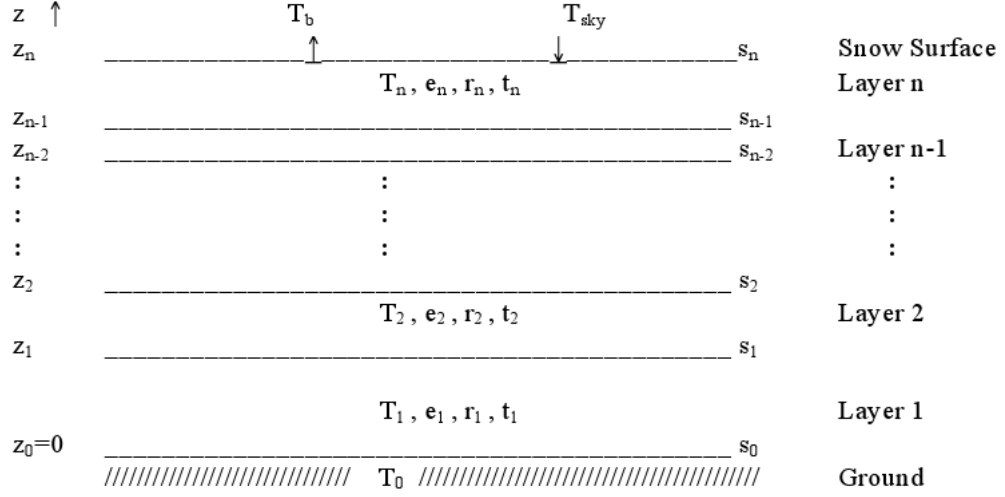
2.2   Multiple layers

Figure 2.7: n layers structure. (Source: MEMLS Note.6s Fig.1)

The sandwich model can be extended to multiple layers as showed in Fig. 2.7 either by MEMLS way or by impedance matching way.

2.2.1   Method used by MEMLS

MEMLS uses an iteration method and treats the parameters in matrix to give an extension to the multiple layers. For each layer, it is characterized by the layer parameters as showed in Fig.2.8. At the boundaries, the brightness
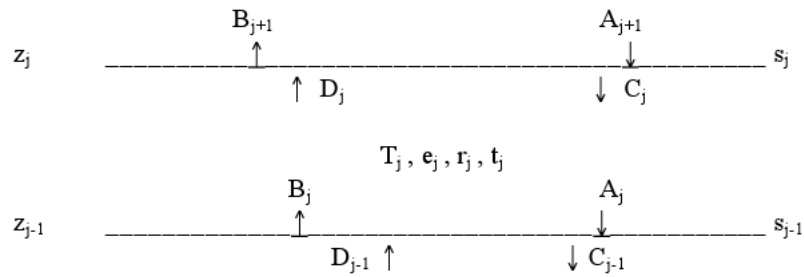

Figure 2.8: The parameters of a selected layer. (Source: MEMLS Note.6s Fig.1)

temperature is related by:

$$A_j = r_j B_j + t_j C_j + e_j T_j$$
$$B_j = s_{j-1} A_j + (1 - s_{j-1}) D_{j-1}$$
$$C_j = (1 - s_j) D_{j+1} + s_j D_j$$
$$D_j = t_j B_j + r_j C_j + e_j T_j$$
$$D_0 = T_0$$
$$A_{n+1} = T_{sky}$$
$$T_b = (1 - s_n) D_n + s_n T_{sky}$$

where j is from 1 to n. Eliminating B_j and C_j, A_j and D_j is expressed as:

$$A_j = r_j[s_{j-1} A_j + (1 - s_{j-1}) D_{j-1}] + t_j[(1 - s_j) A_{j+1} + s_j D_j] + e_j T_j$$
$$D_j = t_j[s_{j-1} A_j + (1 - s_{j-1}) D_{j-1}] + r_j[(1 - s_j) A_{j+1} + s_j D_j] + e_j T_j$$

Witting in form of matrix:

$$\mathbf{A} = \mathbf{M_1}.\mathbf{A} + \mathbf{M_2}\mathbf{D} + \mathbf{E}$$
$$\mathbf{A} = \mathbf{M_3}.\mathbf{A} + \mathbf{M_4}\mathbf{D} + \mathbf{F}$$

Then the upwelling brightness temperature at each layer interface can be achieved by:

$$\mathbf{D} = (\mathbf{I} - \mathbf{M_5})^{-1}.(\mathbf{M_3}.(\mathbf{I} - \mathbf{M_1})^{-1}.\mathbf{E} + \mathbf{D})$$

where

$$\mathbf{D} = \mathbf{M_3}.(\mathbf{I} - \mathbf{M_1})^{-1}.\mathbf{M_2} + \mathbf{M_4}$$

. If there are 2 layers presented, matrix $\mathbf{M_1}, \mathbf{M_2}, \mathbf{M_3}, \mathbf{M_4}$ is:

$$\mathbf{M_1} = \begin{pmatrix} r_1 s_0 & t_1(1 - s_1) \\ 0 & r_2 s_1 \end{pmatrix}$$

$$\mathbf{M_2} = \begin{pmatrix} t_1 s_1 & 0 \\ r_2(1 - s_1) & t_2 s_s \end{pmatrix}$$

$$\mathbf{M_3} = \begin{pmatrix} t_1 s_0 & r_1(1 - s_1) \\ 0 & t_2 s_1 \end{pmatrix}$$

$$\mathbf{M_4} = \begin{pmatrix} r_1 s_1 & 0 \\ t_2(1 - s_1) & r_2 s_s \end{pmatrix}$$

$$\mathbf{E} = \begin{pmatrix} e_1 T_1 + r_1(1 - s_0) T_0 \\ e_4 T_2 + t_2(1 - s_1) T_{sky} \end{pmatrix}$$

$$\mathbf{F} = \begin{pmatrix} e_1 T_1 + t_1(1 - s_0) T_0 \\ e_2 T_2 + r_2(1 - s_1) T_{sky} \end{pmatrix}$$

2.2.2 Impedance matching

Considering the same layer structure as Fig 2.7 but with inverse layer numbering ie increase from top to bottom, for the *ith layer, the radiation contribution of the upward emitted and the downward emitted into the top layer can be derived as:*

$$T_{iU} = \prod_{1 \leq l \leq i-1} (1 - \Gamma_l) T_{Si} \frac{1}{\prod_{2 \leq l \leq i-1} L_l} \prod_{2 \leq l \leq i} \left(\frac{1}{1 - \Gamma(l-1)\Gamma(l)/L_l^2} \right)$$

$$T_{iD} = \prod_{1 \leq l \leq i-1} (1 - \Gamma_l) T_{Si} \Gamma_l \frac{1}{\prod_{2 \leq l \leq i} L_l} \prod_{2 \leq l \leq i} \left(\frac{1}{1 - \Gamma(l-1)\Gamma(l)/L_l^2} \right)$$

where i is from 2 to n. And

$$T_{Si} = (1 - a_i) T_i (1 - \frac{1}{L_i})$$

2.2.3 Comparison

Chapter 3

Translation from physical properties to dielectric constant

Chapter 4

AMSR data

4.1 AMSR introduction

4.2 AMSR data statistical analysis

The AMSR measurement coefficient matrix is given in the Tab.4.1. Fig.4.1 and Fig.4.2 shows the estimated probability density basing on the AMSR data measured during $1^{st}, 1, 2005 - 14^{th}, 1, 2005$ period of location 33 and location 58. The ideal normal distribution with the variance extracted from Tab.4.1 and the average Tb as the mean is plotted together for comparison.

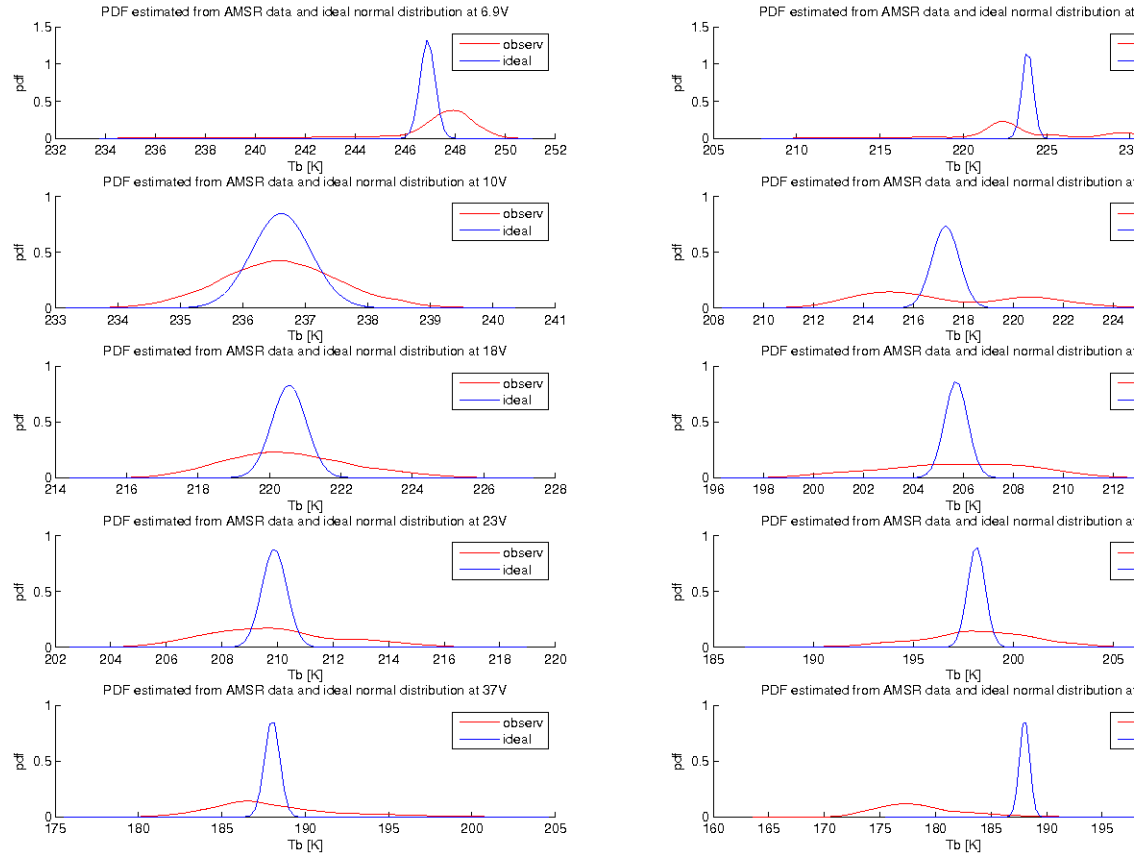| Channel	6GV	6GH	11GV	11GH	19GV	19GH	23GV	23GH	37GV	37GH
6GV	0.09	0	0	0	0	0	0	0	0	0
6GH	0	0.1089	0	0	0	0	0	0	0	0
11GV	0	0	0.2209	0	0	0	0	0	0	0
11GH	0	0	0	0.2916	0	0	0	0	0	0
19GV	0	0	0	0	0.2304	0	0	0	0	0
19GH	0	0	0	0	0	0.2116	0	0	0	0
23GV	0	0	0	0	0	0	0.2025	0	0	0
23GH	0	0	0	0	0	0	0	0.1936	0	0
37GV	0	0	0	0	0	0	0	0	0.2025	0
37GH	0	0	0	0	0	0	0	0	0	0.16

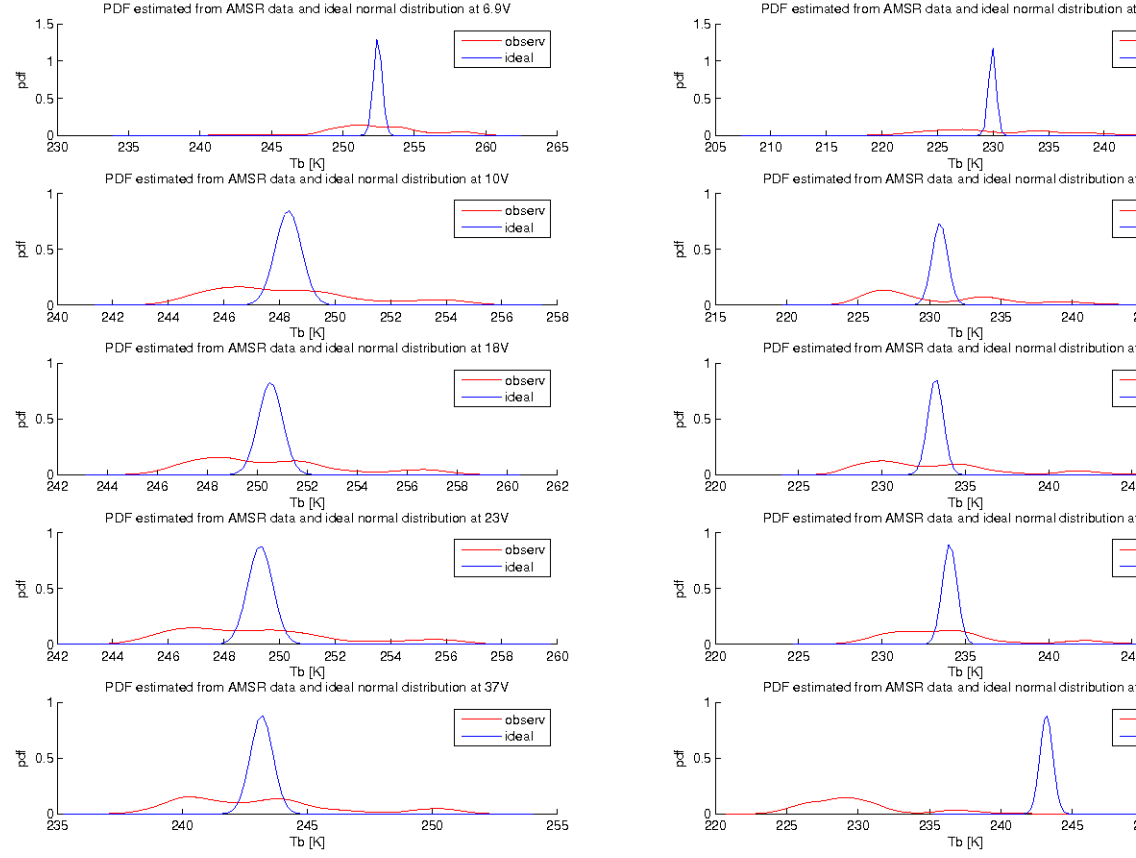Table 4.1: Covariance matrix of AMSR measurements

Figure 4.1: Estimated pdf of AMSR data at location 33.

Figure 4.2: Estimated pdf of AMSR data at location 58